

GRAVITATIONAL-WAVE CONSTRAINTS ON THE COSMIC OPACITY AT $Z \sim 5$: FORECAST FROM SPACE GRAVITATIONAL-WAVE ANTENNA DECIGOSHUAIBO GENG¹, SHUO CAO^{1*}, TONGHUA LIU^{1†}, MAREK BIESIADA², JINGZHAO QI³, YUTING LIU¹, AND ZONG-HONG ZHU¹*Draft version March 17, 2024*

ABSTRACT

Since gravitational waves (GWs) propagate freely through a perfect fluid, coalescing compact binary systems as standard sirens allow to measure the luminosity distance directly and provide distance measurements unaffected by the cosmic opacity. DECi-hertz Interferometer Gravitational-wave Observatory (DECIGO) is a future Japanese space gravitational-wave antenna sensitive to frequency range between target frequencies of LISA and ground-based detectors. Combining the predicted future GW observations from DECIGO and three current popular astrophysical probes (HII regions, SNe Ia Pantheon sample, quasar sample) in electromagnetic (EM) domains, one would be able to probe the opacity of the Universe at different redshifts. In this paper, we show that the cosmic opacity parameter can be constrained to a high precision ($\Delta\epsilon \sim 10^{-2}$) out to high redshifts ($z \sim 5$). In order to reconstruct the evolution of cosmic opacity without assuming any particular functional form of it, the cosmic opacity tests should be applied to individual redshift bins independently. Therefore, we also calculate the optical depth at individual redshifts and averaged $\tau(z)$ within redshift bins. Our findings indicate that, compared with the results obtained from the HII galaxies and Pantheon SNe Ia, there is an improvement in precision when the quasar sample is considered. While non-zero optical depth is statistically significant only for redshift ranges $0 < z < 0.5$, $1 < z < 2$, and $2.5 < z < 3.5$, such tendency is different from that obtained in the framework of its parametrized form. Therefore the importance of cosmic-opacity test without a prescribed phenomenological function should be emphasized.

1. INTRODUCTION

One of the directly observed evidences for Universe undergoing an accelerated expansion at present stage is dimming of type Ia supernovae (SNe Ia) (Riess et al. 1998; Perlmutter et al. 1999). The new component with a negative pressure called dark energy has been proposed to explain the dimming of SNe Ia (Ratra & Peebles 1988; Caldwell et al. 1998; Cao, et al. 2011; Cao & Liang 2013; Cao & Zhu 2014; Ma et al. 2017; Qi et al. 2018) and its nature still remains the biggest problem in cosmology and fundamental physics. This is not the only mechanism which contributes to SNe Ia dimming. Standard astrophysical effects comprise photon absorption or scattering by dust particles in the Milky Way, intervening galaxies or the host galaxy (Tolman 1930; Menard et al. 2010a,b; Xie et al. 2015; Vavryčuk 2019). All of them have been taken into account according to the best of our current knowledge in the preparation of the data sets we used.

In general, any effect that causes the loss or non-conservation of photon number in the beam can contribute to the dimming of distant objects like SNe Ia. Common name for such non-standard or yet unknown mechanisms is cosmic opacity. Some exotic ideas related to cosmic opacity are, for example: conversion of photons into light axions (Csaki et al. 2002; Avgoustidis et al. 2010; Jaeckel & Ringwald 2010) or

gravitons (Chen 1995) in the presence of extragalactic magnetic fields, Kaluza-Klein modes associated with extra-dimensions (Deffayet & Uzan 2000). Up to now, more than 1000 SNe Ia have been detected (Scolnic et al. 2018) and there are the systematic errors rather than statistical ones, which dominate when uses SNe Ia to constrain cosmological parameters. Cosmic opacity might be one source of such systematic errors. Therefore, in the era of precision cosmology it is necessary to accurately quantify any relevant dimming effects.

In the past, the opacity of the universe has been widely investigated by using various astronomical observations (More et al. 2009; Nair et al. 2012; Chen 2012; Li et al. 2013; Holanda et al. 2013; Liao et al. 2013, 2015a; Jesus et al. 2017; Wang et al. 2017). These works generally fall into two categories. The first was to combine the opacity-free angular diameter distances (ADDs) inferred from baryon acoustic oscillations (BAO) or galaxy clusters (More et al. 2009; Nair et al. 2012; Chen 2012; Li et al. 2013) with the luminosity distances (LDs) derived from SNe Ia observations (opacity-dependent). It should be stressed that this approach relies on the so-called “distance duality relation” (DDR) (Etherington 1933, 2007; Cao & Liang 2011). The DDR holds in all cosmological models described by Riemannian geometry and states that LD and ADD should satisfy the relation $D_L = D_A(1+z)^2$, where D_L and D_A are respectively the LD and ADD at the same redshift z . Any deviation from the DDR can contribute to the non-conservation of the photon number (Ellis 2007). Hence, exploring the DDR is equivalent to testing the opacity of the universe, and most of the previous analyses based on currently available D_A data (Cao et al. 2017a,b) still indicated negligible opacity of the Universe. It is obvious that cosmic

¹Department of Astronomy, Beijing Normal University, Beijing 100875, China; *caoshuo@bnu.edu.cn*; *liu_tonghua@mail.bnu.edu.cn*;

²National Centre for Nuclear Research, Pasteura 7, 02-093 Warsaw, Poland

³Department of Physics, College of Sciences, Northeastern University, 110819 Shenyang, China

opacity assessed from the DDR is frequency independent, in contrast to most physically viable mechanisms of opacity affecting D_L measurements. We recommend a detailed discussion of Vavryčuk & Kroupa (2020) concerning cosmic opacity tests based on the DDR. We will come back to this issue in the concluding section.

In the second approach, a cosmological model independent method was proposed by confronting the opacity-independent luminosity distances inferred from the Hubble parameter $H(z)$ measurements of differential ages of passively evolving galaxies (which represent cosmological standard clocks) (Holanda et al. 2013; Liao et al. 2013, 2015a; Jesus et al. 2017; Wang et al. 2017; Liu et al. 2020a) with the (opacity-dependent) luminosity distances of SNe Ia. If universe is opaque, the flux from a standard candle received by the observer will be reduced by a factor $e^{-\tau(z)}$, where $\tau > 0$ is the opacity parameter which represents the optical depth associated to the cosmic absorption.

As an alternative to the above mentioned methods, we will use gravitational waves (GWs) as standard sirens Schutz (1986) to measure directly the opacity-free D_L . Since the first direct detection of the gravitational wave source GW150914 (Abbott et al. 2016), as well as GW170817 (Abbott et al. 2017) with an electromagnetic counterpart identified have opened an era of gravitational wave multi-messenger astronomy (Cao et al. 2019a). In the future one could use the waveform signals of GWs from inspiralling and merging compact binaries to obtain opacity-free LD. Currently, however, due to lack of enough GW events with identified redshifts, extensive efforts have been focused on simulated GW data (Cai et al. 2015; Cai & Yang 2017; Qi et al. 2019a; Wei 2019; Wu et al. 2020). The results of these studies demonstrated that that constraining power of GWs is comparable or better than traditional probes, if hundreds of GW events with the host galaxy identified are available. Recently, Qi et al. (2019a); Wei (2019); Liu et al. (2020b) indicated that GW signals propagate in a perfect fluid with no absorption or dissipation, which means that information about the LDs contained in the GW signals is unaffected by the transparency of the universe. Their work showed that using of GW events from the third generation of GW detector, the Einstein Telescope (ET), has significant potential and natural advantage to test cosmic opacity. In our simulations we focus on GWs signals from the sources with redshift up to $z \sim 5$ accessible to the space-based GW detector-DECi-hertz Interferometer Gravitational wave Observatory (DECIGO) which is a planned Japanese space-based GW antenna (Seto et al. 2001). The objective of DECIGO is to detect various kinds of gravitational waves in the frequency range $0.1 \sim 100$ Hz. Concerning inspiraling compact binaries, they could be detected by DECIGO years before they enter the sensitivity band of ground based detectors. This will open a new window of multifrequency gravitational wave astronomy. We will explore the potential of DECIGO to test the transparency of universe.

For this purpose we additionally need to have independent probes of opacity-dependent LDs extending to such high redshift range. In particular we will consider the following probes. First is the sample of 156 HII galaxies, which includes 25 high- z HII galaxies, 107 local HII

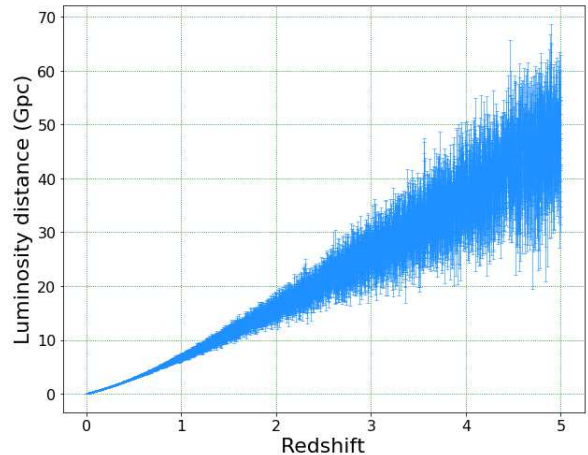


Figure 1. The luminosity distance measurements from 10,000 simulated GW events observable by the space detector DECIGO.

galaxies, and 24 giant extragalactic HII regions covering the range of redshifts $0 < z < 2.33$. Second, we use 1048 newly-compiled SNe Ia data (Pantheon sample) covering the redshift range of $0.07 < z < 2.26$. Another such probe is the sample 1598 the quasar's having UV and X-ray flux measurements spanning the redshift range of $0.036 < z < 5.10$. The purpose of our research is to assess the precision level of opacity constraints which might be achieved using future GW observations from the DECIGO. The paper is organized as follows. The details of simulations of LDs accessible from the GW data from the DECIGO are presented in Section 2. Section 3 introduces the observational data including HII galaxies and HII regions sources, Pantheon sample, and quasars samples. Section 4 presents the cosmic opacity parameterizations used in our study and reveals the results. Finally, we summarize our main conclusions and make a discussion in Section 5.

2. GW STANDARD SIRENS FROM DECIGO

It is well known that GW from inspiraling binaries can be standard sirens (Abbott et al. 2016, 2017). More importantly, since GWs travel in the universe without any absorption or scattering, the LDs derived from GW signals would represent LDs unaffected by cosmic opacity (Qi et al. 2019b; Zhang et al. 2020).

The DECIGO (Seto et al. 2001; Kawamura et al. 2011), or DECi-Hertz Interferometric Gravitational Observatory, is Japan's proposed new mission based on the laser interferometer space satellites. Its advantage is that compared to LIGO, Virgo, ET and the Laser Interferometric Space Antenna (LISA), its scientific goal lies in frequency range of gravitational wave signal, lower than ground based detectors can achieve, but higher than achievable for LISA configuration. Hence the frequency gap between LISA and ground based detectors will be filled. Moreover, GW from the inspiraling and merging compact binaries systems consisting of neutron stars (NSs) and black holes (BHs) can be used to determine the Hubble constant if the redshift of the source is available (Schutz 1986). DECIGO will enable discovery of NS-NS and BH-NS binaries in their inspiral phase long time before they enter the LIGO frequency range. Therefore synergy between DECIGO and ground based detectors

will increase the precision of inferences made from chirp signals (Piórkowska-Kurpas et al. 2020). Signals in the DECIGO band can also be generated from the primordial black holes, facilitating their ultimate detection. In addition, the SNR ratio of DECIGO is much higher than that of current ground-based gravitational wave detectors, so the systematic error caused by observation will be greatly reduced, and the detection limit will be extended to the earlier period in the history of the universe.

The Fourier transform of the GW waveform with a coalescing binary system of masses m_1 and m_2 can be expressed as

$$\tilde{h}(f) = \frac{A}{D_L(z)} M_z^{5/6} f^{-7/6} e^{i\Psi(f)}, \quad (1)$$

where $\Psi(f)$ is the inspiral phase term of the binary system and $A = (\sqrt{6}\pi^{2/3})^{-1}$ is a geometrical average over the inclination angle of a binary system. Here $D_L(z)$ is LD of the source at redshift z and $M_z = (1+z)\eta^{3/5}M_t$ is the redshifted chirp mass, where $M_t = m_1 + m_2$ is the total mass, and $\eta = m_1 m_2 / M_t^2$ is the symmetric mass ratio.

The function $\Psi(f)$ represents the frequency-dependent phase arising from the orbital evolution which can be given by 1.5 (or higher) post-Newtonian (PN) approximation (Maggiore 2008; Cutler & Flanagan 1994; Kidder et al. 1993). Its concrete expression will not affect the final result of luminosity distance calculation, because this term will be eliminated during the detailed calculations. Here we just need to remind that it is a function of the coalescence time t_c , the initial phase of emission ϕ_c , M_z , f and η . There are five unknown parameters, namely: $\theta = \{M_z, \eta, t_c, \phi_c, D_L\}$, where D_L is the LD at redshift z determined from the rate of changing of the frequency f . Following the previous analysis of Sathyaprakash et al. (2010); Zhao et al. (2011), the mass of each neutron star is assumed to be uniformly distributed in the range of $[1, 2] M_\odot$, while the coalescence time and the initial phase of emission are taken as the simplified case of $(t_c, \phi_c) = (0, 0)$. For the purpose of uncertainty estimation we used the Fisher matrix approach. In our case the Fisher matrix has the following form:

$$\Gamma_{ab} = 4Re \int_{f_{min}}^{f_{max}} \frac{\partial_a \tilde{h}_i^*(f) \partial_b \tilde{h}_i(f)}{S_h(f)} df, \quad (2)$$

where ∂_a means derivative with respect to parameter θ_a . DECIGO design assumes the constellation of four equilateral triangular units equipped with detectors at the vertices of triangles. This design is equivalent to eight effective L-shaped detectors (Kawamura et al. 2011; Yagi & Seto 2011), so Γ_{ab} above should be multiplied by 8. The analytical fit of DECIGO noise spectrum (Kawamura et al. 2019, 2006; Nishizawa et al.

2010; Yagi & Seto 2011) is given by

$$\begin{aligned} S_h(f) = & 6.53 \times 10^{-49} \left[1 + \left(\frac{f}{7.36Hz} \right)^2 \right] \\ & + 4.45 \times 10^{-51} \times \left(\frac{f}{1Hz} \right)^{-4} \times \frac{1}{1 + \left(\frac{f}{7.36Hz} \right)^2} \\ & + 4.94 \times 10^{-52} \times \left(\frac{f}{1Hz} \right)^{-4} \text{Hz}^{-1}, \end{aligned} \quad (3)$$

where the three terms on the right hand side represent the shot noise, the radiation pressure noise and the acceleration noise, respectively.

For the purpose of the simulation, we assume the flat Λ CDM universe as our fiducial model. The matter density parameter $\Omega_m = 0.315$ and the Hubble constant $H_0 = 67.4 \text{ km s}^{-1} \text{ Mpc}^{-1}$ from the latest *Planck* CMB observations (Planck Collaboration 2018) are assumed in the simulations. The luminosity distance for a flat Λ CDM universe is

$$D_{L,GW}(z) = \frac{c(1+z)}{H_0} \times \int_0^z \frac{dz'}{\sqrt{\Omega_m(1+z')^3 + (1-\Omega_m)}}. \quad (4)$$

We put GW subscript to denote that it represents opacity-free LD of the source determined with some uncertainty (see below). We then make Monte Carlo simulations of $D_L(z)$ probing the distribution of GW sources. Redshift distribution of GW sources observed on Earth can be written as (Sathyaprakash et al. 2010)

$$P(z) \propto \frac{4\pi D_C^2(z) R(z)}{H(z)(1+z)}, \quad (5)$$

where $H(z)$ and $D_C(z)$ represent the Hubble parameter and the co-moving distance at redshift z , respectively. The NS-NS coalescence rate $R(z)$ is taken the form provided by Cutler & Harms (2006); Schneider et al. (2001).

Concerning the uncertainty, let us remind that the combined SNR for the network of space borne detectors not only helps us confirm the detection of GW with $\rho_{net} > 8$, which is the SNR threshold currently used by LIGO/Virgo network, but also contributes to the error on the luminosity distance as $\sigma_{D_{L,GW}}^{inst} \simeq \frac{2D_{L,GW}}{\rho}$ (Zhao et al. 2011). Meanwhile, the lensing uncertainty caused by the weak lensing should also be taken into consideration. It can be modeled as $\sigma_{D_{L,GW}}^{lens} / D_{L,GW} = 0.05z$ (Sathyaprakash et al. 2010). Therefore, the distance precision per GW is taken as

$$\begin{aligned} \sigma_{D_{L,GW}} &= \sqrt{(\sigma_{D_{L,GW}}^{inst})^2 + (\sigma_{D_{L,GW}}^{lens})^2} \\ &= \sqrt{\left(\frac{2D_{L,GW}}{\rho} \right)^2 + (0.05z D_{L,GW})^2}. \end{aligned} \quad (6)$$

Now the key question is how many GW events can be detected per year in DECIGO. According to Kawamura et al. (2019) summarizing the scientific objectives of DECIGO, 10,000 NSs binary GW signals per year are expected to be detected at redshift ~ 5 based on the frequency of the NS binary coalescences given

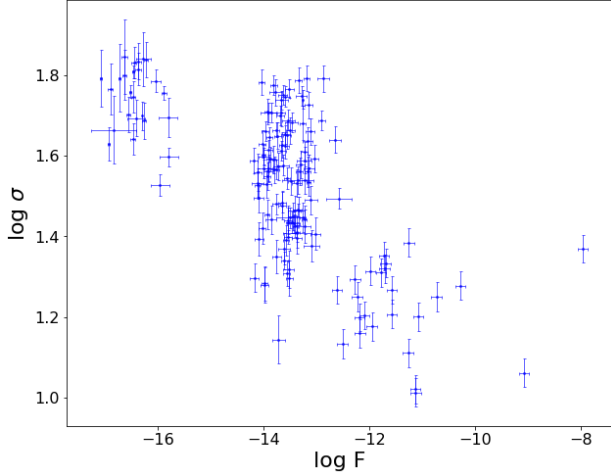


Figure 2. The scatter plot of 156 HII galaxies and extragalactic HII regions (Terlevich et al. 2015), with the reddening-corrected fluxes $\log F(\text{H}\beta)$ and the corrected velocity dispersions $\log \sigma(\text{H}\beta)$.

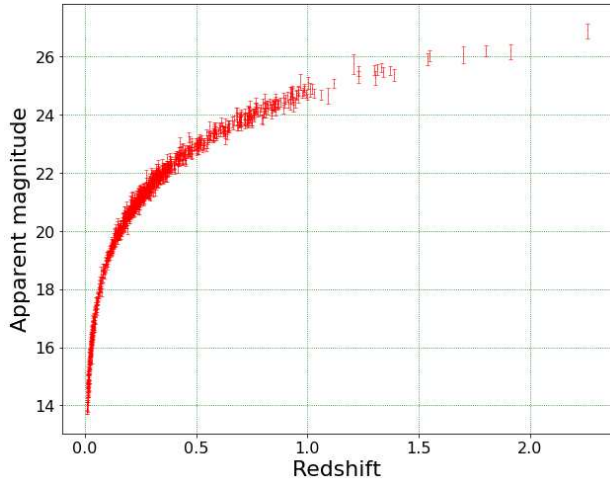


Figure 3. The scatter plot of 1048 SNe Ia in the Pantheon sample (Scolnic et al. 2018), with the measurements of the apparent magnitude in B -band (m_B).

above. Even though GW may provide us some information about the redshift of the source (Messenger & Read 2012; Messenger & Takami 2014), it is not enough to provide accurate redshifts. Therefore, the electromagnetic counterparts are necessary for the redshift determination. Cutler & Holz (2009) demonstrated that it is technologically viable. Thus, we simulate 10,000 GW events and assume that their redshift is known and use this simulation for statistical analysis in the next section. The simulated sample of 10,000 $D_L(z)$ measurements from GW signals detectable by the space detector DECIGO are shown in Fig. 1.

3. OPACITY-DEPENDENT LUMINOSITY DISTANCES IN THE EM DOMAIN

In order to get the opacity-dependent luminosity, we turn to three catalogues of $D_L(z)$ acquired by three different methods separately based on HII galaxies and extragalactic HII region sources, SNe Pantheon sample, and the UV-X ray quasar sample.

3.1. HII galaxies and extragalactic HII regions

The first opacity-dependent LD is inferred from HII galaxies (HIIGx) and giant extragalactic HII regions (GEHR). The existence of HIIGx and GEHR both are explained by star formation theory. A little different than HIIGx, GEHRs are generally located in the outer discs of late-type galaxies, but they form physically similar systems (Melnick et al. 1987). In particular, their total luminosity is almost completely dominated by the starburst episode and optical spectra are indistinguishable. The rapidly forming stars surrounded by hydrogen ionized by massive star clusters emit strong Balmer lines in $\text{H}\alpha$ and $\text{H}\beta$. Possibility of using these galaxies as standard candles lies in the fact that the luminosity $L(\text{H}\beta)$ in $\text{H}\beta$ line is strongly correlated with the ionized gas velocity dispersion σ . The number of energetic photons capable of ionizing hydrogen and the turbulent velocity of the gas both increase with the increasing mass of the starburst component (Terlevich & Melnick 1981).

A well-compiled sample of HII galaxies with accurately measured flux density and the turbulent velocity of the gas could be used as a cosmic distance indicator at redshifts beyond the current reach of SNe Ia (Siegel et al. 2005; Plionis et al. 2011; Wei et al. 2016; Wu et al. 2020; Chávez et al. 2012, 2014; Terlevich et al. 2015). Based on the emission-line luminosity versus ionized gas velocity dispersion relation (called $L-\sigma$ relation), HIIGx and GEHR used as standard candles are suitable for cosmological applications. The relevant form of $L-\sigma$ relation reads:

$$\log L(\text{H}\beta) = \alpha \log \sigma(\text{H}\beta) + \kappa, \quad (7)$$

where α is the slope and κ is intercept. With a well-known expression $L = F \times 4\pi D_L^2$, one can derive LD, as a function of flux F :

$$D_{L,\text{HII}} = 10^{0.5[\alpha \log \sigma(\text{H}\beta) - \log F(\text{H}\beta) + \kappa] - 25.04}. \quad (8)$$

The corresponding uncertainty of $D_{L,\text{HII}}$ can be calculated by error propagation formula:

$$\sigma_{D_{L,\text{HII}}} = (0.5 \ln 10) D_{L,\text{HII}} \sqrt{(\alpha \sigma_{\log \sigma})^2 + (\sigma_{\log F})^2}, \quad (9)$$

where $\sigma_{\log \sigma}$ and $\sigma_{\log F}$ are the observational uncertainties of the (logarithms of) reddening corrected $\text{H}\beta$ flux and the corrected velocity dispersion. However, it should be noted that a zero-point of the original $L-\sigma$ relation is required to assess the model parameters, i.e., α , κ . Numerous efforts have been made to calibrate the zero-point of this relation, for example, Wu et al. (2020) used Hubble parameter $H(z)$ measurements and GW to constrain model parameters. However, in order to avoid introducing more systematic errors in our work, we regard α and κ as statistical nuisance parameters (Wei et al. 2016). Full information about the sample of 156 HII regions that remain after the aforementioned selection can be found in Table 1 of Wei et al. (2016). Fig. 2 shows the total sample of 156 HII source data as a function of redshift ($0 < z < 2.33$), which comprises 25 high- z HIIGx, 107 local HIIGx, and 24 GEHR (Terlevich et al. 2015).

3.2. Type Ia supernovae observation and Pantheon dataset

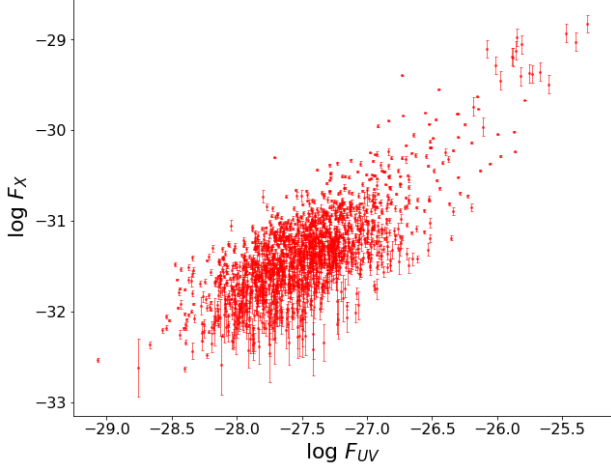


Figure 4. The scatter plot of a sample of 1598 quasars (Risaliti & Lusso 2019), with the available observations of X-ray fluxes $\log(F_X)$ and UV fluxes $\log(F_{UV})$.

The second source of opacity-dependent LDs are SNe Ia. Recently, the Pan-STARRS1 (PS1) Medium Deep Survey has released a dataset (Pantheon) which contains 1048 SNe Ia covering redshift range of $0.01 < z < 2.3$ (Scolnic et al. 2018). The advantage of using this dataset is richness of the sample and its depth in redshift superseding previous datasets like JLA (Betoule et al. 2014). The Pantheon catalogue combines the subset of 279 PS1 SNe Ia Rest & Scolnic (2014); Scolnic et al. (2014) and useful distance estimates of SNe Ia from SDSS, SNLS, various low redshift and HST samples (Scolnic et al. 2018). The distance modulus of SNe Ia can be expressed in following form

$$\mu_{SN} = m_B - M_B + \alpha^* \cdot X_1 - \beta \cdot \mathcal{C}, \quad (10)$$

where m_B is the apparent magnitude in B -band, X_1 is the stretch determined by the shape of the SNe light curve, \mathcal{C} is the color measurement, α^* and β coefficient characterized stretch-luminosity and color-luminosity relationships, respectively. One should note that M_B treated here as nuisance parameter, denotes the absolute magnitude in B -band, whose value is determined by the host stellar mass $M_{stellar}$ by a step function

$$M_B = \begin{cases} M_B^1, & \text{if } M_{stellar} < 10^{10} M_\odot \\ M_B^1 + \Delta M, & \text{otherwise,} \end{cases} \quad (11)$$

Hence, there are four nuisance parameters ($\alpha^*, \beta, M_B^1, \Delta M$) to be fitted. Fortunately, the Pantheon sample is based on the approach called BBC (for BEAMS with Bias Corrections) (Kessler & Scolnic 2017), which is novel with respect to previous SALT2 methodology. Applying the BBC method, Scolnic et al. (2018) reported the corrected apparent magnitude $m_{B,corr} = m_B + \alpha^* \cdot X_1 - \beta \cdot \mathcal{C} + \Delta M$ for all the SNe Ia. Therefore, the observed distance modulus of SNe Ia is simply $\mu_{SN} = m_{B,corr} - M_B$ (Ma et al. 2019). The total uncertainty of distance modulus in the Pantheon dataset can be expressed

$$\sigma_{\mu_{SN}} = \sqrt{\sigma_{m_{B,corr}}^2}, \quad (12)$$

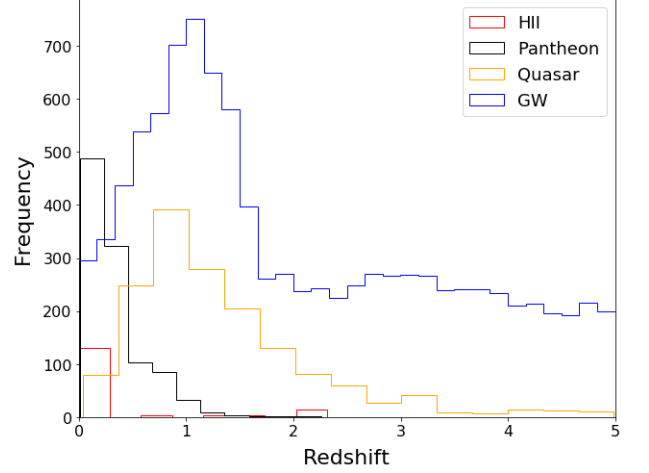


Figure 5. The redshift distribution of NS-NS binaries that would be observed by DECIGO, compared with distribution of EM probes used to derive opacity-dependent luminosity distance.

where $\sigma_{m_{B,corr}}$ is the observational error of the corrected apparent magnitude (see Scolnic et al. (2018) for more details). One can get the LD of SNe Ia in Mpc by a well-known equation

$$D_{L,SN} = 10^{\mu_{SN}/5-5}, \quad (13)$$

and the corresponding uncertainty is

$$\sigma_{D_{L,SN}} = (\ln 10/5) D_L \sigma_{\mu_{SN}}. \quad (14)$$

Fig. 3 shows the SNe Ia data from the most recently compiled Pantheon sample (Scolnic et al. 2018), as a function of redshift ranging from 0.01 to 2.3.

3.3. Nonlinear relation between quasar's X-ray and UV flux measurements

Being the brightest sources in the universe, quasars (QSO) have considerable potential for being useful cosmological probes (Ma et al. 2017; Xu et al. 2018; Cao et al. 2018, 2019b, 2020; Zheng et al. 2020). Unlike SNe Ia, quasars display extreme variability in luminosity and high observed dispersion, which prevents quasars for being a standard candle with a high precision. However, Risaliti & Lusso (2015) through the analysis and refinement of the QSO sample with well measured X-ray and UV fluxes eliminated considerably the contribution of observational dispersion paving the way to make them standard candles. Subsequently, Risaliti & Lusso (2019) collected a sample of 7238 quasars with available X-ray and UV measurements from the cross-correlation of the XMM-Newton Serendipitous Source Catalogue Data Release 7 (Rosen et al. 2016) and the Sloan Digital Sky Survey (SDSS) quasar catalogues from Data Release 7 (Shen et al. 2011) and DR12 (Paris et al. 2017), and then selected 1598 high-quality QSO sample suitable for cosmological applications. Their final results showed that a sample of 1598 quasars with available UV and X-ray observations could produce a Hubble diagram in excellent agreement with that of SNe Ia in the redshift range of ($z < 1.4$) (Liu et al. 2020c). They used a simple nonlinear relation between the X-ray and UV luminosities (Avni & Tananbaum 1986) where X-rays are Compton

scattered photons from an overlying, hot corona and the UV photons are emitted by an accretion disk

$$\log(L_X) = \gamma \log(L_{UV}) + \beta', \quad (15)$$

where L_X and L_{UV} respectively represent the monochromatic luminosity at 2keV and 2500Å in rest-frame, while β' and γ denote the intercept and the slope parameter. With the combination of Eq. (14) and a well-known equation $L = F \times 4\pi D_L^2$, one can derive a LD for each quasar, as a function of the fluxes F , the slope γ , the normalization β

$$D_{L,QSO} = 10^{\frac{1}{2-2\gamma} \times [\gamma \log(F_{UV}) - \log(F_X) + \beta]}, \quad (16)$$

where β is a constant that subsumes the slope γ and the intercept β' , such that $\beta = \beta' + (\gamma - 1) \log 4\pi$. From theoretical point of view, LD can be directly determined from the measurements of the fluxes of F_X and F_{UV} , with a reliable knowledge of the value for the two parameters (γ , β) characterizing the $L_X - L_{UV}$ relation as well as its dispersion. Because the measurement uncertainty of F_{UV} is smaller than the uncertainty of F_X and the global intrinsic dispersion, we therefore neglect it. Thus, the uncertainty of LD from QSO sample is given by

$$\sigma_{D_{L,QSO}} = \ln 10 / (2 - 2\gamma) D_{L,QSO} \sqrt{\sigma_{\log(F_X)}^2 + \delta^2}. \quad (17)$$

The scatter plot of 1598 quasar sample reported by Risaliti & Lusso (2019) is shown in Fig. 4, with the redshift ranging from 0.036 to 5.1.

It should be recalled that the cosmic absorption could affect LD measurements from all the above mentioned probes accessible in the EM window. LD measurements from GWs being unaffected by cosmic opacity, are related to $D_{L,obs}$ representing the LDs derived from HII, SNe, or QSO according to

$$D_{L,obs}(z) = D_{L,GW}(z) e^{\tau(z)/2}. \quad (18)$$

where $\tau(z)$ is the optical depth related to the cosmic absorption. More specifically, if the universe is opaque, the number of photons from sources received by the observer will be reduced, i.e., if $\tau > 0$ which means the reduction of the number of photons.

4. METHODOLOGY AND CONSTRAINED RESULTS OF COSMIC OPACITY

Let us note that all three kinds of probes used to derive opacity-dependent LDs contain model parameters. One possible way to determine their values could be by using external calibrators. However, this might introduce extra systematics and biases, which are hard to quantify. Therefore, in our work, we regard them as free parameters to be optimized along with cosmic opacity parameter ϵ (definition is given below). To be more specific, they are: (α , κ) in the case of HII galaxies and regions, (M_B) in SNe Ia Pantheon sample and (β , γ , δ) in the X-ray - UV quasar sample. Even though this procedure affects the precision of constraints, yet it is a coherent procedure. In order to avoid any bias coming from the redshift differences between opacity-independent and opacity-dependent LDs, we apply the following criterion $|z_{GW} - z_{obs}| < 0.005$, where *obs* represents HII, SNe, or QSO. This redshift selection criterion leads to decrease of the sample sizes. As a result 45 data point are kept

for HII regions, 897 for SNe and 1595 for quasars. The redshift distribution of NS-NS binaries that would be observed by DECIGO is shown in Fig. 5, together with the distribution of three types of EM probes. One can see that current QSO sample has a very similar distribution to future GW data obtainable by DECIGO.

It should be pointed out that, locally transparent universe (at $z = 0$) might be significantly opaque at high redshifts. Such tendency is strongly supported by the observed rate of the damped Ly α absorbers in high-redshift quasars (Prochaska & Herbert-Fort 2004; Rao et al. 2006), as well as the reported abundance of dusty galaxies and dusty halos around star-forming galaxies at $z \sim 7$ (Watson et al. 2015; Fujimoto et al. 2019). Therefore, the cosmic opacity – an integral quantity dependent on the proper dust density, grain-size distribution, and the dust extinction efficiency – could significantly increase with redshifts. In our analysis, such issue is approached in two ways. Firstly, in analogy to previous works of Li et al. (2013); Liao et al. (2013), we assume two particular parameterized forms of the optical depth $\tau(z)$:

$$\begin{aligned} P1 : \tau(z) &= 2\epsilon z, \\ P2 : \tau(z) &= (1 + z)^{2\epsilon} - 1. \end{aligned} \quad (19)$$

If $\epsilon = 0$, it means that photon number is conserved and the universe is transparent. However, one should also be aware of the disadvantage of the first method, i.e., the opacity test just proves whether the opacity follows a specific phenomenological function, as stressed in (Vavryčuk & Kroupa 2020). Therefore, in the subsequent analysis the optical depth will also be studied in individual redshift bins, in order to perform the opacity test in a more generalized way and show how decisive conclusions about the transparency of the universe can be deduced from such tests.

In order to constrain the nuisance parameters and the cosmic opacity parameter simultaneously, we use Python Markov Chain Monte Carlo (MCMC) module, emcee (Foreman-Mackey & Hogg 2013), to obtain the best fitted values and corresponding uncertainties by minimizing the χ^2 objective function defined as

$$\chi^2 = \sum_1^i \frac{[D_{L,GW}(z_i; \epsilon) - D_{L,obs}(z_i; \mathbf{p})]^2}{\sigma_{D_L}(z_i)^2}, \quad (20)$$

where the \mathbf{p} collectively denote nuisance parameters of respective model, $\sigma_{D_L}^2 = \sigma_{D_{L,GW}}^2 + \sigma_{D_{L,obs}}^2$, $\sigma_{D_{L,GW}}$ and $\sigma_{D_{L,obs}}$ are given by Eq. (5) and Eqs. (8), (13), (16), respectively.

In Fig. 6, we plot the one-dimensional marginalized distributions and two-dimensional constraint contours for the opacity parameter ϵ with HII regions nuisance parameters (α , κ) in the P1 and P2 parametrizations. In the P1 case, we obtain $\epsilon = 0.016^{+0.037}_{-0.036}$ with the model nuisance parameters $\alpha = 3.966^{+0.283}_{-0.261}$ and $\kappa = 35.112^{+0.426}_{-0.465}$ at 68.3% confidence level. The 1σ confidence region constraint on cosmic opacity ϵ in P2 case is $\epsilon = 0.013^{+0.063}_{-0.071}$. Our results show that simulated GW data tested against HII regions reaching to redshift $z < 2.316$, support the transparent universe in each parameterized function of optical depth $\tau(z)$. Using different parametrizations of

Parameterized form+Sample	ϵ	α	κ	M_B	β	γ	δ
P1+HII	$0.016^{+0.037}_{-0.036}$	$3.966^{+0.283}_{-0.261}$	$35.112^{+0.426}_{-0.465}$	\square	\square	\square	\square
P2+HII	$0.013^{+0.063}_{-0.071}$	$3.924^{+0.278}_{-0.254}$	$35.175^{+0.416}_{-0.453}$	\square	\square	\square	\square
P1+SN	$0.006^{+0.009}_{-0.009}$	\square	\square	$-19.414^{+0.008}_{-0.008}$	\square	\square	\square
P2+SN	$0.009^{+0.012}_{-0.013}$	\square	\square	$-19.415^{+0.009}_{-0.008}$	\square	\square	\square
P1+QSO	$0.056^{+0.032}_{-0.036}$	\square	\square	\square	$7.550^{+0.408}_{-0.408}$	$0.623^{+0.014}_{-0.014}$	$0.231^{+0.004}_{-0.004}$
P2+QSO	$0.110^{+0.058}_{-0.080}$	\square	\square	\square	$7.526^{+0.423}_{-0.423}$	$0.624^{+0.015}_{-0.014}$	$0.231^{+0.004}_{-0.004}$

Table 1

Results from three types of GW+EM data combinations: the best-fitted value and 68% C.L. of ϵ and other nuisance parameters in two cosmic-opacity parameterizations.

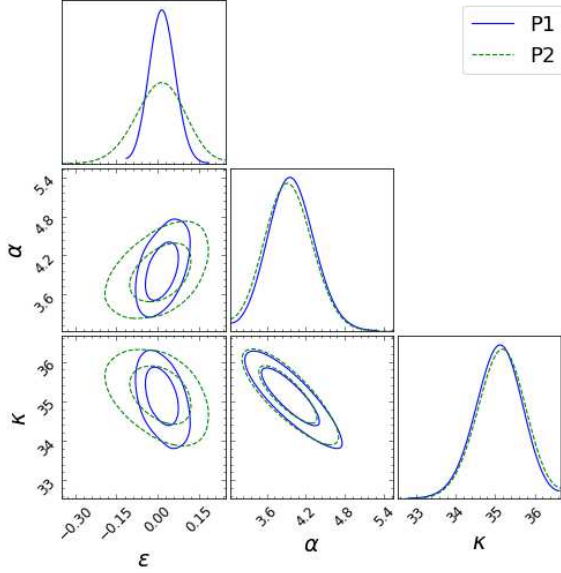


Figure 6. One-dimensional distributions and two-dimensional constraint contours for cosmic opacity parameter ϵ and HII regions nuisance parameters (α , κ) in both P1 (blue dashed line) and P2 parametrization (green solid line).

optical depth yields slightly different constraints of the cosmic opacity ϵ and model nuisance parameters. In the P1 case GW data from the DECIGO would be able to constrain cosmic transparency with the precision of $\Delta\epsilon \sim 0.04$. It is worth remembering that due to our redshift pre-selection a sample of only 45 HII regions were used here to combine with GW events from the DECIGO. More interestingly, we find that our constraints on the nuisance parameters (see Table I) are different from those results of Wu et al. (2020): $\alpha = 5.17 \pm 0.09$, $\kappa = 32.86 \pm 0.12$, which are derived from a calibration by simulated GW events in a flat Λ CDM cosmology. The main reason for the difference is that only 45 HII regions samples are used here rather than 156 sources in work of Wu et al. (2020). The other reason may be due to the covariance between cosmic opacity and the nuisance of HII regions, which can be seen from the constraint contours.

One should bear in mind that, an accurate reconstruction of $\tau(z)$ can considerably improve our understanding of the nature of cosmic opacity. In order to reconstruct the evolution of $\tau(z)$ without any prior assumption of its specific functional form, we calculate the optical depth from Eq. (18) at individual redshifts and average $\tau(z)$ within redshift bins. Fig. 7 shows the resulting optical depth. One can see that no statistically significant evidence of deviation from the transparent universe

($\tau(z) = 0$) can be detected from low-redshift HII galaxies. Yet, interestingly, the HII region data favors a transition from $\tau = 0$ at low redshift to $\tau > 0$ at higher redshift, a behavior that is consistent with the true optical depth increasing with redshifts. Such tendency, which is different from that obtained in the framework of parameterized form, is supported by the recent works of Ma & Corasaniti (2018); Vavryčuk & Kroupa (2020) stressing the importance of cosmic-opacity test without a prescribed phenomenological function.

The results derived from the simulated GW events from DECIGO and Pantheon sample are shown in Fig. 8 and Table I. One can see that almost transparent universe is also favored up to redshift $z < 2.26$: the best fitted value of ϵ with 1σ C.L. is 0.006 ± 0.009 and 0.009 ± 0.012 for P1 and P2 cases, respectively. Compared with previous work, Qi et al. (2019a) combined simulated GW events from the ET with Pantheon SNe Ia to test the opacity of the Universe, they results shown that the best-fit values with 1σ standard error for cosmic opacity is 0.009 ± 0.016 with the absolute magnitude $M_B = -19.4 \pm 0.016$ in P1 case ($\epsilon = 0.015 \pm 0.025$ and $M_B = -19.404 \pm 0.019$ in P2 case). Although their results are consistent with our work (not only ϵ , but also M_B), our finding suggest that the future space-based GW detector DECIGO could result in more stringent constraints on the transparency of the universe than the ET. Meanwhile, the optical depth $\tau(z)$ is also calculated by combining the simulated GW events and the current SNe Ia observations at individual redshift bins, with the final results displayed in Fig. 7. Benefit from the large sample size of the Pantheon SNe Ia sample, the cosmic opacity can be constrained with higher precision. As can be seen from individual points of $\tau(z)$ as well as for its binned values, the optical depth without any parameterized form show that the universe is transparent within 1σ C.L. However, we also find that a redshift bin shifts the confidence interval for $\tau(z = 0.5)$ towards large optical depth, which might be overlooked by the cosmic-opacity test in a prescribed phenomenological function.

The use of the QSO sample extending up to $z \sim 5$, in combination with GW data supposed to be obtainable in DECIGO, enables us to probe the transparency of the universe at much earlier stages of its evolution. Fig. 9 displays the constraint results on cosmic opacity ϵ with quasar nuisance parameters (β , γ , δ) in the P1 and P2 cases. For the first P1 parametrization form, we obtain $\epsilon = 0.056^{+0.032}_{-0.036}$, $\beta = 7.550^{+0.408}_{-0.408}$, $\gamma = 0.623^{+0.014}_{-0.014}$, $\delta = 0.231^{+0.004}_{-0.004}$ where upper and lower number denote 68% confidence region. For the second P2 parametrization

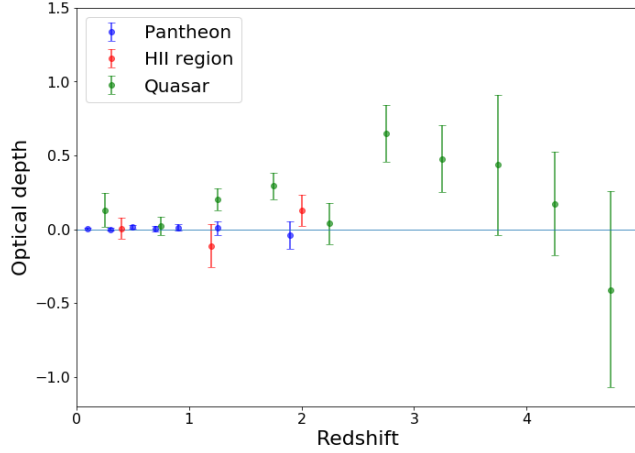


Figure 7. Optical depth calculated from the combinations of available EM observations and the GW sample observed by DECIGO: the binned optical depth with the 68.3% confidence intervals corresponding to the redshift bins of [0, 0.8, 1.6, 2.4] for HII region sample, the redshift bins of [0, 0.2, 0.4, 0.6, 0.8, 1.0, 1.5, 2.3] for the SNe Ia Pantheon sample, and the redshift bins of [0, 0.5, 1.0, 1.5, 2.0, 2.5, 3.0, 3.5, 4.0, 4.5, 5.0] for the quasar sample.

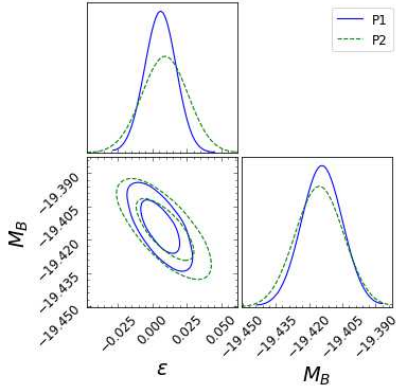


Figure 8. One-dimensional distributions and two-dimensional constraint contours for cosmic opacity parameter ϵ and SNe Ia nuisance parameters (M_B), using the Pantheon sample and simulated GW dataset.

form, the results are $\epsilon = 0.110^{+0.058}_{-0.080}$, $\beta = 7.526^{+0.423}_{-0.423}$, $\gamma = 0.624^{+0.015}_{-0.014}$, $\delta = 0.231^{+0.004}_{-0.004}$. Our results indicate that current observations of QSOs confronted with simulated opacity-free LDs from GW signals do not suggest any significant deviation from the transparency of the universe. A transparent universe is supported by the future GW dataset simulated from the DECIGO and quasars flux measurements within 2σ confidence level. One can clearly see that using quasars sample with the different parameterized forms for optical depth result with significantly different central values of ϵ than HII regions or the Pantheon sample. Qi et al. (2019a) suggested that the dependence of test cosmic opacity on the optical depth parameterization chosen for is relatively weak. This was because the redshift range explored in their work was only up to $z \sim 2.3$, while in our case it is $z \sim 5$. The two parameterized forms P1 and P2 are approximately equal at low redshifts, but at high redshifts they diverge. Our results highlights the importance of choosing a reliable parameterization for $\tau(z)$ in order to better check the cosmic opacity validity at much high redshift. Although our best fitted central value of cosmic opacity parameter has some deviation from $\epsilon = 0$, yet the quasars' nuisance parameters are consistent at 1σ confidence level with the results of Melia (2019), which were

obtained within the flat Λ CDM cosmology. More importantly, our findings show a strong degeneracy between the opacity parameter ϵ and quasars nuisance parameters β and γ . A little change in β or γ , will change the value of opacity parameter ϵ noticeably. This covariance is similar to that seen in the SNe Ia. Therefore, using an independent reliable external calibrator to calibrate quasar's nuisance parameter becomes particularly important. In order to make the opacity test to more general, optical depth is also studied in individual redshift bins by combining quasar sample and simulated GW events from DECIGO. The results are shown in Fig. 7. Compared with the results obtained from the HII galaxies and Pantheon SNe Ia, there is a noticeable improvement in precision when the quasar sample is considered. More importantly, we obtain that non-zero optical depth is statistically significant only for redshift bins $0 < z < 0.5$, $1 < z < 2$, and $2.5 < z < 3.5$. More data extending to the above redshifts will be necessary to investigate the cosmic opacity in this high-redshift region where the uncertainty is still very large.

In order to highlight the advantages of our work, it is worthwhile to compare our results with the previous analysis performed to test the cosmic opacity with actual or expected tests involving the LDs from various astrophysical probes. In the work of Wei (2019), the authors combined the GW observations of a third-generation GW detector – ET with SNe Ia data Pantheon sample in similar redshift ranges to test cosmic opacity. Their results shown that the cosmic opacity parameter $\Delta\epsilon \sim 0.026$ (at 68.3% confidence level) for P1 function with 1000 simulated GW events, and they concluded that using GW standard sirens and SNe Ia standard candles yields the results competitive with previous works. Moreover, Qi et al. (2019a) performed the same test of cosmic opacity as Wei (2019) did. Differently, Qi et al. (2019a) considered not only the Pantheon sample but also the JLA sample. Combining luminosity distances from joint light-curve analysis (JLA) and simulated GW events from ET, they got $\epsilon = 0.002 \pm 0.035$ for P1 parametrization and $\epsilon = -0.0060 \pm 0.053$ for P2 case, respectively. It is necessary to mention that although we expect ten thousand GW signals from DECIGO detectable, yet after match-

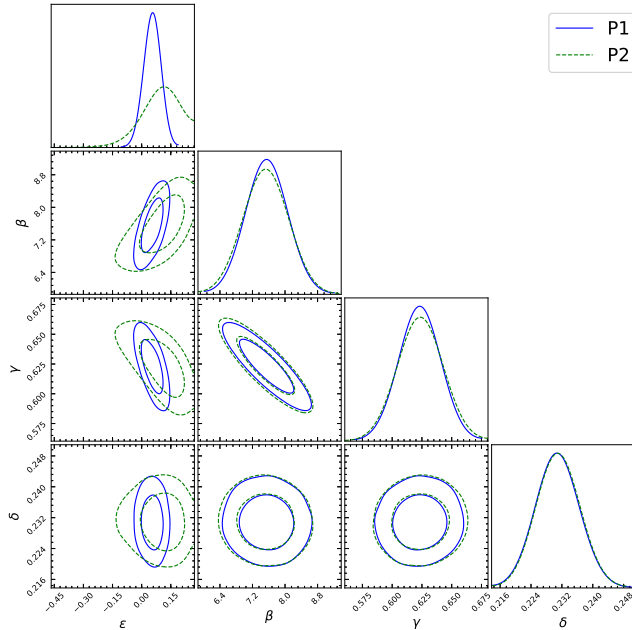


Figure 9. One-dimensional distributions and two-dimensional constraint contours for cosmic opacity parameter ϵ and quasar nuisance parameters (β , γ , δ), using the QSO sample and simulated GW dataset.

ing with the Pantheon sample, only about 1000 GW signals satisfy the redshift selection criteria, which is about the same number as in the works of Wei (2019); Qi et al. (2019a). By comparing the results at 1σ confidence level, we obtain the uncertainty smaller by 65% than these of Wei (2019) in the P1 case with Pantheon dataset. Comparing to Qi et al. (2019a), uncertainties of our results are 75% and 78% smaller than their in the P1 and P2 case, respectively. Such stringent constraints are a result of the DECIGO data having much higher SNR than the ET, hence the uncertainties of the LDs inferred are smaller. Therefore, using GW signals from the DECIGO may achieve higher precision of the measurements of cosmic opacity than the other popular astrophysical probes.

5. CONCLUSIONS AND DISCUSSION

In this paper, we proposed a new model-independent cosmological test for the cosmic opacity at redshifts up to $z \sim 5$. We combined opacity-free LDs inferred from simulated GW events representative to the space-based GW detectors of DECIGO with three popular astrophysical probes used to derive the opacity-dependent LDs. The GW signals propagate in a perfect fluid without any absorption or dissipation, which means that the information about LDs contained in the GW signals is unaffected by the transparency of the universe. Such high redshift range has never been explored by previous works. We adopted two parameterization forms to describe the optical depth $\tau(z)$ describing the cosmic absorption.

Different from the previous works, we not only used SNe Ia as standard candles to obtain opacity-dependent LD, but also HII regions sources based on $L-\sigma$ relation and quasar flux measurements based on nonlinear relation in X-ray and UV bands acting standard candles. Considering the calibration of nuisance parameters occurring typically in standard candles, we treated them as free parameters optimized along with cosmic opacity

parameter. One of the purposes of our research is to what extent can one test the transparency for our universe if DECIGO detects a certain number of GW events.

In the case of HII regions serving as standard candles, the redshift selection resulted with only 45 HII regions data points left and used to constrain cosmic opacity. The cosmic opacity parameter ϵ was constrained with the precision is 0.04 and 0.07 in P1 and P2 cases, respectively. Compared with previous papers, such as Li et al. (2013), who used two galaxy cluster samples and the Union2.1 to constrain cosmic opacity resulting with $\epsilon = 0.009 \pm 0.057$ for P1 case and $\epsilon = 0.014 \pm 0.070$ for P2, our results shown that HII regions have powerful potential to get more stringent constraint on cosmic opacity. On the other hand, we shown that just 45 GW events from the DECIGO can constrain the cosmic opacity parameter with high accuracy. More interestingly, our constraints on the HII regions nuisance parameters (α , κ) are somewhat different from recent results of Wu et al. (2020). In the case of SNe Ia Pantheon sample, the cosmic opacity can be constrained with higher precision: the uncertainty can be further reduced to $\Delta\epsilon \sim 0.010$, and the absolute magnitude uncertainty can be reduced to $\Delta\epsilon \sim 0.016$, which is consistent with the previous works (Wei 2019; Qi et al. 2019a). By comparing our results with previous opacity constraints, we prove that our method using GW signals from space-based DECIGO detector as standard sirens and SNe Ia standard candles will be competitive.

The third cosmological probe we used was a carefully selected sample of QSOs whose X-ray and UV fluxes are measured and which are promising new class of standard candles. Combining QSOs with simulated GW events, our result show that, there is no large deviation from a transparency of the Universe within 2σ confidence level. The cosmic opacity parameter was constrained with an accuracy $\Delta\epsilon \sim 10^{-2}$. Due to the lack of convincing form of parameterization for τ at such high redshift, or any reliable theoretical suggestion for it, two parameterizations (Li et al. 2013; Liao et al. 2013) were used in our work. We demonstrated that the cosmic opacity results were slightly sensitive to the parameterization form assumed. This emphasizes the importance of choosing a reliable parameterization form for $\tau(z)$ at much high redshift. Moreover, our findings illustrate that there is a strong degeneracy between the cosmic opacity parameter ϵ and quasars nuisance parameters (β , γ) which may affect the real the value of the cosmic opacity parameter. The independent external calibration of quasars nuisance parameters is therefore particularly important. In order to reconstruct the evolution of $\tau(z)$ without assuming any specific functional form of it, the cosmic opacity tests should be applied to individual redshift bins independently. Therefore, in this paper we calculated the optical depth at individual redshifts and averaged $\tau(z)$ within redshift bins. Our findings indicated that, compared with results obtained from the HII galaxies and Pantheon SNe Ia, there is an improvement in precision when the quasar sample is considered, while non-zero optical depth is statistically significant only for redshifts $0 < z < 0.5$, $1 < z < 2$, and $2.5 < z < 3.5$.

It should be pointed out that according to the recent analysis of Vavryčuk (2019); Vavryčuk & Kroupa (2020), the cosmic opacity could vary with frequency since it strongly depends on wavelength according to the

extinction law (Mathis 1990; Li & Draine 2001; Draine 2003). The problem was recognized a long time ago (Aguirre 2000; Corasaniti 2006), with a heuristic suggestion that the luminosity distance data sets covering different frequencies might be differently sensitive to the transparency of the universe (Vavryčuk & Kroupa 2020). In our analysis, we combined the predicted future GW observations from DECIGO with three types of EM data (HII regions, SNe Ia Pantheon sample, quasar sample), and furthermore checked whether these EM data can be affected by cosmic opacity in different ways. Considering the fact that X-ray photons can destroy dust grains instead of being absorbed, physically different processes could be detected from the observations of X-ray fluxes, instead of simple luminosity dimming due to dust absorption of low-energy photons (Draine & Hao 2002; Morgan et al. 2014). Our final results showed that the cosmic opacity could attain different values for different types of D_L data covering different wavelengths (optical for HII regions, SNe Ia Pantheon sample, ultraviolet for quasar sample), although such effect is still difficult to be precisely quantified (see Vavryčuk & Kroupa (2020) for a detailed discussion). Thus, the goal of our test is not just to check the resolution power of the GW data, but also to assess the performance of the combination of current and future available data in gravitational wave (GW) and electromagnetic (EM) domain. Let us also comment on the issue raised by Vavryčuk & Kroupa (2020), that combining the GW data with other types of data (SNe Ia, QSO, HII galaxies) should be avoided since these data can be affected by cosmic opacity in a different way, because the cosmic opacity is strongly frequency dependent. While this point of view is in principle true, one can argue in the following way: the data sets of cosmological probes like standard candles have been prepared according to the best available knowledge concerning possible opacity sources. In particular, Risaliti & Lusso (2019) have considered the (differential) absorption in UV and X-ray bands while constructing their sample. Then, after checking against opacity-free probes like standard rulers or GW standard sirens, by using the DDR relation (the fundamental one, but frequency independent) one could be able to find the evidence for unaccounted opacity sources, or at the very least the new physics involved. This is the idea behind our approach.

As a final remark, we have successfully constrained the cosmic opacity covering the redshift range $0 < z < 5$. Although the constraint on cosmic opacity by using quasars X-ray and UV flux measurements did not improve the results obtained with HII regions or SNe Ia, it provided an insight into cosmic opacity at an earlier stage of the universe. Our results demonstrate the huge potential of standard candles and GW signals – standard sirens to measure cosmic opacity at high redshifts. Current GW detectors did not allowed us yet to make such inferences, however in the near future the data we were forced to simulate will become a daily experience of now emerging GW astronomy. It would be fruitful to prepare for this era and suggest which problems could be addressed then with high accuracy. Cosmic opacity issue certainly belongs to this class of problems.

ACKNOWLEDGMENTS

We would like to thank the referee for constructive comments, which allowed to improve the paper substantially. This work was supported by National Key R&D Program of China No. 2017YFA0402600; the National Natural Science Foundation of China under Grants Nos. 12021003, 11690023, 11633001, and 11373014; Beijing Talents Fund of Organization Department of Beijing Municipal Committee of the CPC; the Strategic Priority Research Program of the Chinese Academy of Sciences, Grant No. XDB23000000; the Interdiscipline Research Funds of Beijing Normal University; and the Opening Project of Key Laboratory of Computational Astrophysics, National Astronomical Observatories, Chinese Academy of Sciences. J.-Z. Qi was supported by China Postdoctoral Science Foundation under Grant No. 2017M620661, and the Fundamental Research Funds for the Central Universities N180503014. M.B. was supported by the Foreign Talent Introducing Project and Special Fund Support of Foreign Knowledge Introducing Project in China. He was supported by the Key Foreign Expert Program for the Central Universities No. X2018002.

REFERENCES

- Abbott, B. P., et al. [LIGO Scientific and Virgo Collaborations], 2016, PRL, 116, 061102
- Abbott, B. P., et al. [LIGO Scientific Collaboration, the Virgo Collaboration], 2017, PRL, 119, 161101
- Aguirre, A. N. 2000, ApJ, 533, 1
- Avgoustidis, A., Burrage, C., Redondo, J., Verde L., & Jimenez, R. 2010, JCAP, 10, 024
- Avni, Y. & Tananbaum, H. 1986, ApJ, 305, 83
- Betoule, M., et al. 2014, A&A, 568, 22
- Caldwell, R., et al. 1998, PRL, 80, 1582
- Cao, S., & Liang, N. 2011, RAA, 11, 1199
- Cao, S., Liang, N., & Zhu, Z.-H. 2011, MNRAS, 416, 1099
- Cao, S., & Liang, N. 2013, IJMPD, 22, 1350082
- Cao, S., & Zhu, Z.-H. 2014, PRD, 90, 083006
- Cao, S., Zheng X., Biesiada M., Qi J., Chen Y. & Zhu Z.-H. 2017a, A&A, 606, A15
- Cao, S., Biesiada, M., Jackson, J., Zheng, X. & Zhu Z.-H. 2017b, JCAP, 02, 012
- Cao, S., et al. 2018, EPJC, 78, 749
- Cao, S., et al. 2019a, NatSR, 9, 11608
- Cao, S., et al. 2019b, PDU, 24, 100274
- Cao, S., et al. 2020, ApJL, 888, L25
- Cai, R.-G., et al. 2016, PRD, 93, 043517
- Cai, R.-G. & Yang, T. 2017, PRD, 95, 044024
- Chávez, R., et al. 2012, MNRAS, 425, L56
- Chávez, R., et al. 2014, MNRAS, 442, 3565
- Chen, P. 1995, PRL, 74, 634
- Chen, J., Wu, P., Yu, H., & Li, Z. 2012, JCAP, 10, 029
- Corasaniti, P. S. 2006, MNRAS, 372, 191
- Csaki, C., et al. 2002, PRL, 88, 161302
- Cutler, C. & Flanagan, E. E. 1994, PRD, 49, 2658
- Cutler, C. & Harms, J. 2006, PRD, 73, 042001
- Cutler, C. & Holz, D. E. 2009, PRD 80, 104009
- Deffayet, C. & Uzan, J.-P. 2000, PRD, 62, 063507
- Draine, B. T. & Hao, L. 2002, ApJ, 569, 780
- Draine, B. T. 2003, ARA&A, 41, 241
- Ellis, G. F. R. 2007, Gen. Rel. Grav., 39, 1047
- Etherington, I. M. H. 1933, Phil. Mag., 15, 761
- Etherington, I. M. H. 2007, Gen. Rel. Grav., 39, 1055
- Foreman-Mackey, D., Hogg, D. W., Lang, D., & Goodman, J. 2013, PASP, 125, 306
- Fujimoto, S., et al. 2019, ApJ, 887, 107
- Holanda, R. F. L., et al. 2013, JCAP, 1304, 027
- Jaackel, J., & Ringwald, A. 2010, Ann. Rev. Nucl. Part. Sci. 60, 405
- Jesus, J. F., Holanda, R. F. L., & Dantas, M. A. 2017, General Relativity and Gravitation, 49, 150

- Kawamura, S., Nakamura, T., Ando., M. et al., 2006, CQG, 23, 125
- Kawamura, S., Nakamura, T., Ando., M. et al., 2019, IJMPD, 28, 1845001
- Kawamura, S., et al. 2011, CGQ, 28, 094011
- Kessler, R., & Scolnic, D. 2017, ApJ, 836, 56
- Kidder, L. E., Will, C. M., & Wiseman, A. G. 1993, PRD, 47, 3281
- Li, Z., et al. 2013, PRD, 87, 103013
- Li, A. & Draine, B. T. 2001, ApJ, 554, 778
- Liao, K., et al. 2013, PLB, 718, 1166
- Liao, K., et al. 2015a, PRD, 92, 123539
- Liu, Y. T., et al. 2020a, ApJ, 901, 129
- Liu, T. H., et al. 2020b, ApJ, 899, 71
- Liu, T. H., et al. 2020c, MNRAS, 496, 708
- Ma, Y.-B., et al. 2017, EPJC, 77, 891
- Ma, C. & Corasaniti, P.-S. 2018, ApJ, 861, 124
- Ma, Y.-B., et al. 2017, EPJC, 77, 891
- Ma, Y.-B., et al. 2019, ApJ, 887, 163
- Maggiore, M. Gravitational Waves, 2008, Oxford University Press, New York
- Mathis, J. S. 1990, ARA&A, 28, 37
- Melia, F. 2019, MNRAS, 489, 517
- Melnick, J., Moles, M., Terlevich, R., Garcia-Pelayo, J.-M., 1987, MNRAS, 226, 849
- Menard, B., Scranton, R., Fukugita, M., & Richards, G. 2010a, MNRAS, 405, 1025
- Menard, B., Kilbinger, M., & Scranton, R. 2010b, MNRAS, 406, 1815
- Messenger, C. & Read, J. 2012, PRL, 108, 091101
- Messenger, C., Takami, K., Gossan, S., Rezzolla, L., & Sathyaprakash, B. S. 2014, PRX, 4, 041004
- More, S., et al. 2009, ApJ, 696, 1727
- Morgan, A. N., et al. 2014, MNRAS, 440, 1810
- Nair, R., Jhingan, S., & Jain, D. 2012, JCAP, 12, 028
- Nishizawa, A., Taruya, A., & Kawamura, S. 2010, PRD, 81, 104043
- Paris, I., et al. 2017, A&A, 597, 79
- Perlmutter, S., et al. 1999, ApJ, 517, 565
- Piórkowska-Kurpas, A., et al. 2020, ApJ, submitted [arXiv:2005.08727]
- Aghanim, N., Akrami, Y., Ashdown, M., et al. [Planck Collaboration] 2018, arXiv:1807.06209
- Plionis, M., et al. 2011, MNRAS, 416, 2981
- Prochaska, J. X. & Herbert-Fort, S. 2004, PASP, 116, 622
- Qi, J.-Z., et al. 2018, RAA, 18, 66
- Qi, J. Z., et al. 2019a, PRD, 100, 023530
- Qi, J. Z., et al. 2019, PDU, 26, 100338
- Rao, S. M., Turnshek, D. A., & Nestor, D. B. 2006, ApJ, 636, 610
- Ratra, B., & Peebles, P. E. J. 1988, PRD, 37, 3406
- Rest, A., Scolnic, D., Foley, R. J., et al. 2014, ApJ, 795, 44
- Riess, A. G., et al. 1998, AJ, 116, 1009
- Risaliti, G., & Lusso, E. 2015, ApJ, 815, 33
- Risaliti, G., & Lusso, E. 2019, Nature Astronomy, 3, 272
- Rosen, S. R., et al. 2016, A&A, 590, 1
- Sathyaprakash, B., et al. 2010, CQG, 27, 215006
- Schutz, B. F. 1986, Nature, 323, 310
- Scolnic, D., Rest, A., Riess, A., et al. 2014, ApJ, 795, 45
- Scolnic, D., et al. 2018, ApJ, 859, 101
- Schneider, R., et al. 2001, MNRAS, 324, 797
- Seto, N., Kawamura, S., & Nakamura, T. 2001, PRL, 87, 221103
- Shen, Y. et al. 2011, ApJS, 194, 45
- Siegel, E. R., et al. 2005, MNRAS, 356, 1117
- Terlevich, R. & Melnick, J., 1981, MNRAS, 195, 839
- Terlevich, R., et al. 2015, MNRAS, 451, 3001
- Tolman, R. C. 1930, Proc. Natl. Acad. Sci., 16, 511
- Vavryčuk, V. 2019, MNRAS, 489, L63
- Vavryčuk, V. & Kroupa, P. 2020, MNRAS, 497, 378
- Wang, G.-J., Wei, J.-J., Li, Z.-X., Xia, J.-Q., & Zhu, Z.-H. 2017, ApJ, 847, 45
- Watson, D., et al. 2015, Nature, 519, 327
- Wei, J.-J., Wu, X.-F., & Melia, F. 2016, MNRAS, 463, 1144
- Wei, J.-J. 2019, ApJ, 876, 1
- Wu, Y., et al. 2020, 888, 113
- Xie, X., Shen, S., Shao, Z., & Yin, J. 2015, ApJ, 802, L16
- Xu, T., et al. 2018, JCAP, 06, 042
- Yagi, K. & Seto, N. 2011, PRD, 83, 044011
- Zhao, W., Van Den Broeck, C., Baskaran, D., & Li, T. 2011, PRD, 83, 023005
- Zhang, S., et al. 2020, IJMPD, in press [arXiv:2009.04204]
- Zheng, X., et al. 2020, ApJ, 892, 103